

Remote preparation of a single-mode photonic qubit by measuring field quadrature noise

S. A. Babichev, B. Brezger, A. I. Lvovsky[*]

Fachbereich Physik, Universität Konstanz, D-78457 Konstanz, Germany

(Dated: April 1, 2022)

An electromagnetic field quadrature measurement, performed on one of the modes of the nonlocal single-photon state $\alpha|1,0\rangle - \beta|0,1\rangle$, collapses it into a superposition of the single-photon and vacuum states in the other mode. We use this effect to implement remote preparation of arbitrary single-mode photonic qubits conditioned on observation of a preselected quadrature value. The quantum efficiency of the prepared qubit can be higher than that of the initial single photon.

Remote state preparation (RSP) is a quantum communication protocol which allows indirect transfer of quantum information between two distant parties by means of a shared entangled resource and a classical channel. Unlike the celebrated teleportation scheme [1], the sender (Alice) does not possess a copy of the source state, but is aware of its full classical description. To implement RSP, she performs a measurement on her share of the entangled resource in a basis chosen in accordance with the state she wishes to prepare. Dependent on the result of her measurement, the entangled ensemble collapses either onto the desired state at the receiver (Bob's) location, or can be converted into it by a local unitary operation.

Although RSP has been formulated [2] and investigated theoretically [3] as a quantum communication protocol only recently, its concept can be traced back to the seminal work of Einstein, Podolsky, and Rosen (EPR) [4], who have considered an entangled state of two particles with correlated positions and momenta. By choosing to measure either the position or the momentum of her particle, Alice can remotely prepare Bob's particle in an eigenstate of either observable, thus instantaneously creating either of two mutually incompatible physical realities at a remote location.

Aside from many experiments on the EPR paradox, both in the original [5] and in the Bohm-Bell [6] configurations, controlled collapse of an entangled wavepacket has been utilized experimentally to prepare a single photon by means of conditional measurements on a photon pair generated via parametric down-conversion. When a single-photon detector, located in one of the emission channels, registers a photon, the entangled pair state collapses into a single photon in a well-defined spatiotemporal mode travelling along the other emission channel. This technique was proposed in 1986 [7] and has since been employed in many experiments.

In most theoretical and experimental work on controlled state collapse, the observable measured by Alice coincided with the one that defines the entanglement basis. Upon the measurement, the EPR state will collapse into an eigenstate of this observable. If Bob measures the same observable as Alice, his result will be highly correlated with Alice's.

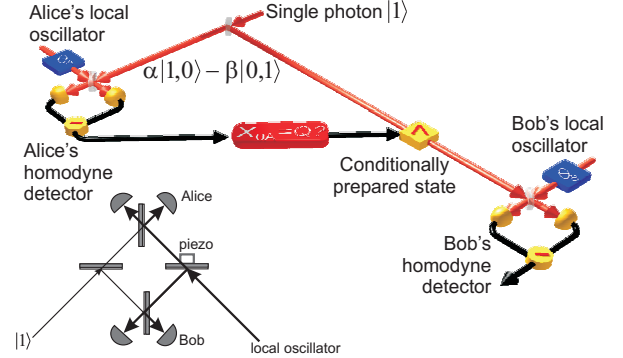


FIG. 1: a) Scheme of the experiment. A photon incident on a beam splitter generates a nonlocal single-photon state. Alice performs a quadrature measurement using her homodyne detector, thus preparing a state $x|0\rangle + y|1\rangle$ at Bob's location. Inset: Schematic of the actual experimental arrangement. The four beam splitters must be kept interferometrically stable with respect to each other.

In the experiment reported here, such a straightforward correlation is not present. We start with a two-mode optical state entangled in the photon number (Fock) basis, $|\Psi\rangle = \alpha|1\rangle_A|0\rangle_B - \beta|0\rangle_A|1\rangle_B$. To perform RSP, Alice measures the quantum noise of the electric field quadrature observable $\hat{X}_{\theta A}$, which is only weakly correlated in this ensemble. A particular result obtained by Alice does not mean that Bob, by measuring the same observable, would acquire the same (or similar) value. Yet, as we demonstrate, the RSP scheme is fully functional: the measurement by Alice collapses the EPR state into a pure single-mode photonic qubit $x|0\rangle + y|1\rangle$.

In other words, we prepare a bit of quantum information encoded in a *discrete* (photon number) basis by measuring a *continuous* observable (field quadrature). So far, discrete- and continuous-variable quantum information science has developed with little overlap between these two domains. One of the main messages of this Letter is that these two subfields are in fact closely intertwined and that a number of novel phenomena can be observed at their interface.

Other work investigating this interface include theo-

retical proposals to improve the degree of squeezing in a two-mode squeezed state [8] and generating Schrödinger-cat states [9]. Foster *et al.* performed a cavity QED experiment in which detection of a photon coming out of a cavity prepared an optical state with a well-defined phase [10].

A *conceptual scheme* of our experiment is shown in Figure 1. A single photon $|1\rangle$ incident upon a beam splitter with transmission α^2 and reflection β^2 generates the entangled state $|\Psi\rangle$ which is shared between Alice and Bob. With each incoming photon, Alice performs a homodyne measurement on her part of the entangled state with the local oscillator set to a preselected phase θ_A . If her measurement result is equal to a preselected value Q (which we call *conditional quadrature*), she notifies Bob via a classical channel. Upon receipt of Alice's message, Bob performs a homodyne measurement of his fraction of $|\Psi\rangle$ to characterize the remotely prepared state.

Alice's homodyne measurement is associated with the quadrature operator

$$\hat{X}_{\theta A} = \hat{X} \cos \theta_A + \hat{P} \sin \theta_A, \quad (1)$$

\hat{X} and \hat{P} being the canonical position and momentum observables. By detecting a particular quadrature value $X_{\theta A} = Q$, Alice projects the entangled resource $|\Psi\rangle$ onto a quadrature eigenstate $\langle Q_{\theta A}|$:

$$\begin{aligned} |\psi_B\rangle &= \mathcal{N} \langle Q_{\theta A} | \Psi \rangle \\ &= \mathcal{N} [\alpha \langle Q_{\theta A} | 1 \rangle_A |0\rangle_B - \beta \langle Q_{\theta A} | 0 \rangle_A |1\rangle_B], \end{aligned} \quad (2)$$

which is just a coherent superposition of the single-photon and vacuum states

$$|\psi_B\rangle = x |0\rangle + y |1\rangle \quad (3)$$

with $x = \mathcal{N} \alpha \langle Q_{\theta A} | 1 \rangle$ and $y = -\mathcal{N} \beta \langle Q_{\theta A} | 0 \rangle$ (\mathcal{N} is a normalization factor). These coefficients are the well known stationary solutions of the Schrödinger equation for a particle in a harmonic potential [11]:

$$\langle Q_{\theta} | 0 \rangle = \left(\frac{2}{\pi} \right)^{1/4} e^{-Q^2}; \quad (4)$$

$$\langle Q_{\theta} | 1 \rangle = 2 \left(\frac{2}{\pi} \right)^{1/4} Q e^{-i\theta} e^{-Q^2}. \quad (5)$$

By choosing particular values of θ and Q , Alice can remotely prepare any random vector on the surface of the Bloch sphere.

In our *experiment* the initial single-photon state was prepared by means of a conditional measurement on a biphoton produced via parametric down-conversion. We used frequency-doubled 2-ps pulses from a mode-locked Ti:Sapphire laser running at $\lambda = 790$ nm which underwent down-conversion in a BBO crystal, in a type-I frequency-degenerate, but spatially non-degenerate configuration. A single-photon detector (Perkin-Elmer),

placed into one of the outcoming channels, detected biphoton creation events and triggered the quantum communication protocol described above. A more detailed description of our laser setup can be found in Refs. [12, 13].

The actual geometric arrangement of the RSP apparatus is shown in the inset to Fig. 1. The experiment required high interferometric stability of all modes involved, so the distance between Alice's and Bob's stations had to be minimized. Because the single-photon state has no optical phase, only the relative phase between Alice's and Bob's modes $\theta_A - \theta_B$ has a physical meaning and affects the homodyne statistics. We have therefore chosen to control this difference directly rather than each phase individually. This was done by means of a piezoelectric transducer as shown in the figure.

The local oscillator pulses for homodyne detection have been provided by the master Ti:Sapphire laser. Their spatiotemporal modes had to match the respective modes of the nonlocal single-photon state. Mode matching was optimized via the technique described in [12], i.e. by simulating the single photon by a classical pulse and maximizing the visibility of the interference with the local oscillators at each beam splitter.

Optical losses, dark counts of the trigger detector, and non-ideal mode matching result in some distortion of the RSP scheme. Fortunately, almost all these imperfections can be accounted for by assuming that the single photon entering the first beam splitter has some admixture of the vacuum state:

$$\hat{\rho}_{|1\rangle} = |1\rangle\langle 1| + (1 - \eta) |0\rangle\langle 0| \quad (6)$$

where $\eta_{|1\rangle}$ is the cumulative quantum efficiency incorporating the imperfections of the entire apparatus. It can be evaluated by independent reconstruction of optical ensembles arriving to each homodyne detector. Both Alice's and Bob's ensembles are statistical mixtures of the type (6), with the single photon fractions of $\alpha^2 \eta$ and $\beta^2 \eta$, respectively. We found $\eta = 0.55$ [14]. Note that Eq. (6) is valid even though some of the losses occur *after* the photon has been split into two modes.

Regarding inefficiencies according to Eq. (6), we write the remotely prepared ensemble as

$$\hat{\rho}_B = E |\psi_B\rangle\langle\psi_B| + (1 - E) |0\rangle\langle 0| \quad (7)$$

where $|\psi_B\rangle$ is given by Eq. (3) and the qubit preparation efficiency is

$$E = \frac{\eta(\alpha^2 \langle Q|1\rangle^2 + \beta^2 \langle Q|0\rangle^2)}{\eta(\alpha^2 \langle Q|1\rangle^2 + \beta^2 \langle Q|0\rangle^2) + (1 - \eta) \langle Q|0\rangle^2}. \quad (8)$$

The "success rate", i.e. the fraction of those events in which $X_{\theta A}$ approximates Q , is proportional to

$$R = (1 - \eta) \langle Q|0\rangle^2 + \eta \alpha^2 \langle Q|1\rangle^2 + \beta^2 \langle Q|0\rangle^2. \quad (9)$$

Our *data acquisition* procedure was based on postselection. Homodyne measurements at Bob's station were performed every time, independent of Alice's result. We varied the relative phase $\theta_A - \theta_B$ slowly and with each incoming photon, acquired a pair of values $(X_{\theta_A}, X_{\theta_B})$ from both homodyne detectors. Then we selected those pairs for which X_{θ_A} approximated a particular conditional quadrature Q within a certain margin of error (Fig. 2) and reconstructed the optical ensemble associated with the respective Bob's data.

For reconstruction, we utilized the novel likelihood-maximization method [15]. This technique, previously not applied to experimental homodyne tomography, warrants a higher reconstruction fidelity than the inverse Radon transformation employed traditionally, and ensures physical plausibility of the reconstructed ensemble. A detailed description of the reconstruction procedure will be published elsewhere.

We have executed two data acquisition runs using two different beam splitters with transmission α^2 equal to 0.5 and 0.08. With each beam splitter, a large data set of about 300,000 points was acquired for a full relative phase cycle. The data were binned up according to the value of X_{θ_A} with the bin size of 0.071, except the last two bins which were twice as wide. Maximum-likelihood estimation of Bob's ensembles associated with each bin yielded density matrices in the Fock basis. As expected, all matrix elements except ρ_{00} , ρ_{01} , ρ_{10} , and ρ_{11} were negligibly small. This allowed us to interpret the reconstructed ensembles in accordance with Eq. (7), i.e. as a statistical mixture of the state $|\psi_b\rangle$ and the vacuum, and to evaluate the qubit value $|y^2|$ and its preparation efficiency E for each postselected subset of the experimental data. The success rate is given by the relative size of each subset. These quantities, along with their theoretical predictions, are plotted in Fig. 3. Good agreement between theory and experiment is achieved, except for relatively high Q values where the preparation rate is reduced and so are the respective data subsets.

Fig. 3(a) shows that the fraction $|y^2|$ of the single photon in the qubit decreases with increasing conditional quadrature Q . This is easily interpreted by reviewing the vacuum and single-photon wavefunctions (4) and (5). The quadrature probability density associated with the single-photon state is generally broader than that of the vacuum and vanishes at $Q = 0$. If Alice detects $X_A = 0$, she can tell with certainty that her mode is in the vacuum state and the photon must have been reflected to Bob. On the contrary, detection of a large quadrature value by Alice is much more likely if her mode contains a photon — and Bob's does not.

As evidenced by Fig. 3, a highly reflective ($\alpha^2 = 0.08$) beam splitter provides a more profitable preparation rate and efficiency for qubits with a high single-photon fraction (low Q) than a symmetric beam splitter. For qubits with a high vacuum fraction the relation is inverse. This

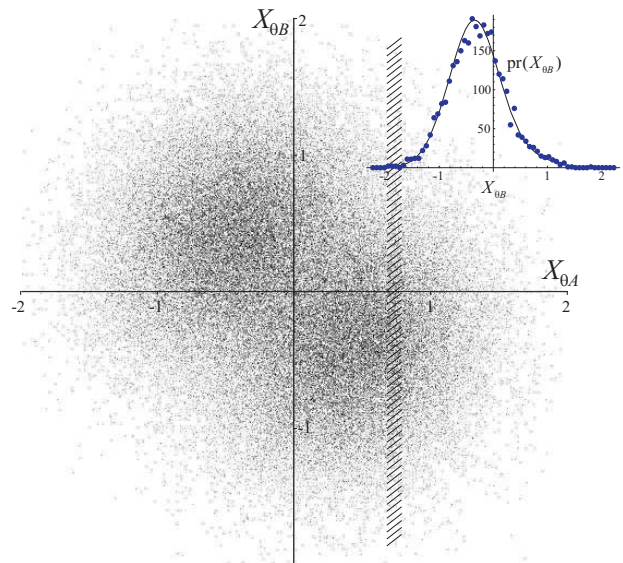


FIG. 2: 61440 samples of homodyne measurements by Alice and Bob acquired for $\theta_A - \theta_B = 0$. Although both parties measure the same quadrature, the quantum noise exhibits little correlation. Inset: a histogram of Bob's data conditioned on $X_{\theta_A} = 0.71$ (shaded area of the main plot). This is one of the marginal distributions of the Wigner function in Fig. 4(b).

is further illustrated in Fig. 4 where experimental Wigner functions of two ensembles prepared using different beam splitters and Q values are plotted.

One surprising feature associated with the protocol is that the preparation efficiency E of the remotely prepared state can be *higher* than the efficiency of the initial single photon as long as the conditional quadrature value Q exceeds $1/2$ (Fig. 3(c)). In other words, the reported scheme features not only preparation, but also, for qubits with a sufficiently high vacuum fraction, *purification* of the prepared qubit [16]. In quantum-optical experiments at visible wavelengths the vacuum state is readily available; still it appears surprising that this “free” vacuum can be incorporated into the prepared qubit in a controlled, coherent manner.

The observed purification effect raised our curiosity about a possibility of extension to single photons. Can one distill a high-purity single-photon state from a large set of mixtures (6) with moderate efficiency? This problem is relevant to a variety of recently reported solid-state sources which are capable of generating single photons “on demand” but in a poor spatiotemporal mode [17]. Purification would make such sources applicable to the linear optical quantum computation scheme [18].

In conclusion, we have reported remote state preparation of single-mode photonic quantum bits in a counterintuitive scheme. We started with a two-mode quantum state with the entangled *discrete* degree of freedom

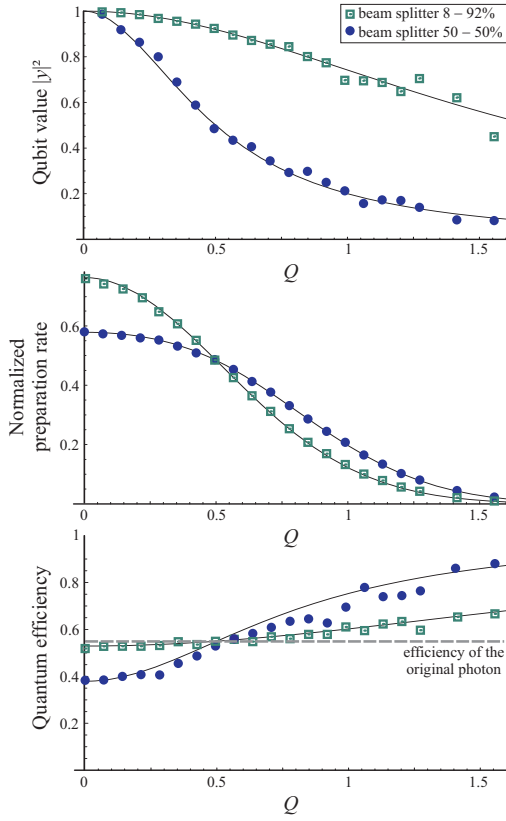


FIG. 3: (a) Single-photon fraction $|y|^2$ in the qubit as a function of the preselected quadrature Q . With a symmetric beam splitter, values of Q below $1/2$ correspond to a prepared state with a single photon fraction greater than 50 percent. (b) Relative success rate of remote state preparation. (c) Quantum efficiency of the remotely prepared state. For $Q > 1/2$ the efficiency of the output state is higher than that of the initial single photon.

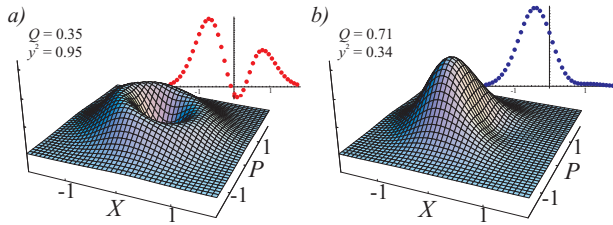


FIG. 4: Examples of Wigner functions of the remotely prepared ensembles reconstructed from the experimental data. (a): $Q = 0.35$, highly reflective beam splitter; (b): $Q = 0.71$, symmetric beam splitter. Insets show cross-sections through symmetry planes.

(number of photons), and by measuring a *continuous* observable (field quadrature) in one of the modes collapsed the entangled state into a coherent superposition of two Fock states in the other mode, again in the *discrete* domain. Surprisingly, the quantum efficiency of the prepared qubit can be higher than that of the initial photon.

This experiment demonstrates, in our opinion, the potential of combining discrete and continuous variable techniques in quantum information technology applications.

We thank the Deutsche Forschungsgemeinschaft and the Optik-Zentrum Konstanz for support.

-
- [*] URL: <http://www.uni-konstanz.de/quantum-optics/quantech/>
- [1] C. H. Bennett *et al.* Phys. Rev. Lett. **70**, 1895 (1993); D. Bouwmeester *et al.*, Nature (London) **390**, 575 (1997); D. Boschi *et al.*, Phys. Rev. Lett. **80**, 1121 (1998); A. Furusawa *et al.*, Science **282**, 706 (1998).
 - [2] H. K. Lo, Phys. Rev. A **62** 012313 (2000); C. H. Bennett *et al.*, Phys. Rev. Lett. **87**, 77902 (2001).
 - [3] A. K. Pati Phys. Rev. A **63**, 014302 (2001); M. G. A. Paris quant-ph/0209168; C. H. Bennett *et al.*, quant-ph/0307100.
 - [4] A. Einstein, B. Podolsky and N. Rosen, Phys. Rev. **47**, 777 (1935).
 - [5] Z. Y. Ou *et al.*, Phys. Rev. Lett. **68**, 3663 (1992); Y. Zhang, K. Kasai, and M. Watanabe, Opt. Lett. **27**, 1244 (2002); W. P. Bowen *et al.*, Phys. Rev. Lett. **90**, 043601 (2003); J. Laurat *et al.*, quant-ph/0304111.
 - [6] J. S. Bell, Physics **1**, 195 (1964); M. A. Rowe *et al.*, Nature **409**, 791 (2001) and references therein.
 - [7] C. K. Hong and L. Mandel, Phys. Rev. Lett. **56**, 58 (1986); P. Grangier, G. Roger and A. Aspect, Europhys. Lett. **1**, 173 (1986)
 - [8] T. Opatrny, G. Kurizki, D.G. Welsch, Phys. Rev. A **61**, 032302 (2000); P.T. Cochrane, T.C. Ralph, G.J. Milburn, Phys. Rev. A **65**, 062306 (2002); J. Eisert *et al.*, quant-ph/0307106
 - [9] M. Dakna *et al.*, Phys. Rev. A **55**, 3184 (1997).
 - [10] G.T. Foster *et al.* Phys. Rev. Lett. **85**, 3149 (2000);
 - [11] Eqs. (4) and (5) for an arbitrary quadrature (1) follow from the properties of the phase-space rotation operator $\hat{U}(\theta) = e^{-i\theta\hat{n}}$. From $\hat{U}^\dagger(\theta)\hat{a}\hat{U}(\theta) = \hat{a}e^{-i\theta}$ we find for the quadrature operator $\hat{U}^\dagger(\theta)\hat{X}\hat{U}(\theta) = \hat{X}_\theta$ and for its eigenstate $|Q_\theta\rangle = \hat{U}^\dagger|X\rangle$. From the first and last relations above, we obtain $\langle n|Q_\theta\rangle = e^{i\theta n}\langle n|X\rangle$. The quantity $\langle n|X\rangle$ is the energy eigenwavefunction of a harmonic oscillator.
 - [12] A. I. Lvovsky *et al.*, Phys. Rev. Lett. **87**, 050402 (2001); T. Aichele, A. I. Lvovsky and S. Schiller, Eur. Phys. J. **D 18**, 237 (2002).
 - [13] A. I. Lvovsky, J. H. Shapiro, Phys. Rev. A **65**, 033830 (2002).
 - [14] A reduction from the value $\eta = 0.62$ reported in some of our earlier papers [13] might be caused by a replacement of our pulsed laser by one with a poorer spatial mode.
 - [15] J. Řeháček, Z. Hradil, and M. Ježek, Phys. Rev. A **63**, 040303 (2001); K. Banaszek *et al.*, Phys. Rev. A **61**, 010304 (1999).
 - [16] J.I. Cirac *et al.*, Phys. Rev. Lett. **82**, 4344 (1999)
 - [17] J. Kim *et al.*, Nature **397**, 500 (1999); P. Michler *et al.*, Science **290**, 2282 (2000).
 - [18] E. Knill, R. Laflamme, G. J. Milburn, Nature (London) **409**, 46 (2001)